scientific reports

Check for updates

OPEN

Bio-sensing applications of a 2:1 photonic crystal multiplexer

Esmat Rafiee

In this work, a two-dimensional ring-shaped photonic crystal structure is proposed. The proposed structure is consisted of 28*25 silicon rods situated in air medium. Fundamental properties of the proposed structure (acting as a biosensor) are investigated through photonic bandgap (PBG) and field distribution diagrams. The proposed structure is considered for diagnosis of cholesterol and creatinine levels in blood samples. Proposed structure is designed to operate as a 2:1 multiplexer (also functioning as a biosensor). Thus, by inserting incident signals with specific wavelengths (placed in TE PBG region) to input0, input1 and select ports, light wave can be transmitted to output port. Cholesterol concentrations in blood sample can be detected by considering input0 ($I_0 = 1$), input1 ($I_1 = 0$) and select (S = 0). For cholesterol following bio sensing factors will be calculated. *Q*: (45.4–52.88), *S*: 2673.4 nm/RIU, *DL*: (0.00125–0.00143) RIU, *FOM*: (80.91–82.06) RIU^{-1}. Creatinine levels in blood samples can also be diagnosed by considering input0 ($I_0 = 0$), input1 ($I_1 = 1$) and select (S = 1). For creatinine, *Q*: (101.1–109.4), *S*: 3582.7 nm/RIU, *DL*: (4.98e–4–5.26e–4) *RIU* and *FOM*: (199.01–201.3) RIU^{-1} will be calculated. Finally, proposed system can effectively help physician in early and precise prognosis of hypercholesterolemia and acute kidney injuries.

Keywords Acute kidney injury, Biosensor, Cholesterol, Creatinine, Multiplexer, Photonic crystal

Recently, optical configurations have been extensively considered in the designation process of different structures (with various applications like bio-optical[1], bio-chemical[2] and other configurations). The progressing and considerably increasing usage of optical configurations are due to their very compact size (integration), lower cost (total fabrication cost in large amounts compared with conventional structures), remarkable high capacities and processing speeds (due to properties of light). The mentioned advantages mainly occur due to the existence of photons in optical-based structures (as known in electronic-based devices electron play the main role while in optical one's photons are responsible for the operating principles)[3–5]. Therefore, designation, fabrication and utilization of optical-based devices have been extensively increased. Thus, in order to design an optical-based device, all of the its elements should be operated based on the optical principles (should be designed based on basic structures like plasmonic[6], graphene[7], plasmonic-graphene[8], photonic crystal[9] and other configurations). As a result, all circuit elements like transmitters, receivers, filters, gates, sensors and multiplexers (MUX) would be designed based on different optical configurations[10–12]. There are many optical configurations that can be considered for the designation process like plasmonic[13], graphene[14], photonic crystal and other structures. Photonic crystal (PhC) based devices have been interesting to scientist due to their simplicity (operation and fabrication), low cost and remarkable efficiency[15]. Photonic crystals are made of periodic dielectric, plasmonic-dielectric or graphene-dielectric microstructures or nanostructures that can affect electromagnetic wave propagation in the structure. PhC structures can be found in nature, like the iridescent colors seen in certain butterflies and opal gemstones (opal is made of 3D PhCs based on small particles of hydrated silica)[16].

PhC based structures can be periodically (circular, hexagonal and cubic) considered in one, two or three dimensions and are consisted of two or more media (mostly dielectric)[17]. Refractive indices introduce characteristics of utilized media in PhC based structures (define behavior of light in defined media)[18]. PhC based structures can be considered by defining periodic cells (rods) in a specific substrate (background which is mostly made of air). The periodicity (the distance between the center of one rod to another (adjacent rods)) can be introduced by a defined factor named as lattice constant[19]. Photonic band gap (PBG) is an essential parameter for defining functionality of a PhC based structure. This factor which can be extracted from the PBG diagram can indicate the permitted (guided) and non-permitted (forbidden) transmitting regions (indicating frequencies or wavelengths). In fact, in the permitted wavelengths, light can move in the structure while in the forbidden regions it can't be transferred. PBG figure can be achieved through applying PWE method to the designed system. Incident light waves have different behaviors in the allowed and non-allowed wavelength ranges. In guided region (wavelengths), light wave would be transferred along PhC system. It will be gradually dispersed (very low amounts of incident light wave can reach the output). In another case, in non-allowed region, light

Department of Electrical Engineering, Faculty of Engineering, Alzahra University, Tehran, Iran. email:

wave cannot be transferred along PhC system. It will be reflected when touching any rod (reflection process would be continuously happened along the PhC structure). This phenomenon (which happens for the forbidden wavelengths) can be considered as the total internal reflection (TIR) effect which defines signal movement in optical based deceives with very low losses (like PhC, plasmonic, graphene and other configurations)[20–24]. As stated, all of the device's elements should be considered based on optical configurations for designing optical integrated circuits (OICs). As known, PhC-based systems can be experimentally fabricated and implemented[25]. Deep ultraviolet lithography, e-beam etching, nano-replica molding and embossing with a template are some of the fabrication methods. Nano-replica molding method is the most economical, effective and flexible fabrication method[26]. Fabrication process steps can be defined in the following part. First, silicon grating template should be prepared. In the second step, surface treatment of the silicon template with hydrophobic silane (or other materials) would happen. After that, spin-coating PDMS would take place. Then, PDMS nano grating would be done. Finally, high refractive index grating film layer through e-beam evaporation would be applied[26].

Optical biosensors can be considered as important and essential elements in optical-based devices. They are extensively utilized in OICs due to their compatibility, integrability, high speed and other specifications[27]. Optical biosensors can be considered based on PhC structures for detection of different bio molecules[28,29]. As stated, concentrations of biological elements such as cholesterol, glucose, hemoglobin, creatinine and other biomolecules could be detected by optical biosensors. Hemoglobin and glucose concentrations can help researchers for prognosis of anemia and diabetes[30]. Unusual levels (high) of cholesterol and creatinine will enhance risks of hypercholesterolemia (which can cause heart diseases and strokes) and acute kidney injuries[31]. Thus, diagnosis of cholesterol and creatinine in blood could aid researchers and patients in prevention, prognosis and treatment of mentioned diseases effectively and with very low costs. In research[32], by considering a 1-D hyperbolic PhC, cholesterol detecting sensor was proposed. Sensitivity, detection limit and FOM of 469 nm/RIU, 0.0091 and 125 RIU^{-1} were obtained. Research[33], by considering an octagonal PhC fiber (PCF) detected cholesterol concentrations. In[34], cholesterol could be detected by considering a biosensor based on GO/PPy/PANI/ZnO nanocomposite. Acceptable sensitivity, detection limit and FOM were obtained. In[31], a biosensor for detection of creatinine concentration was proposed in the shape of 1-D PhC based structure made of MgF_2 and CeO_2 materials. Maximum sensitivity of 306.25 nm/RIU was achieved. In[35], a system made of silver, phosphorous and graphene in various shapes (T-shaped, U-shaped and split ring-shaped waveguides) was designed for prognosis of creatinine in blood samples. Suggested biosensor showed sensitivity of 1562.5 nm/RIU. In this research, an applicable, highly functionalized and easy fabricated structure (2:1 MUX) based on 2-D PhC system is designed for diagnosis of cholesterol and creatinine in blood. Proposed structure is consisted of 28*25 silicon rods in air background. Refractive indices of silicon and air are 3.5 and 1, respectively. In the proposed structure, only linear rods (with various radii) are utilized which facilitate the fabrication and designation processes.

PBG spectrum and field distribution diagrams will be extracted. Finally, designed MUX will be utilized as a bio-sensing device for diagnosis of cholesterol and creatinine. It should also be noted that, fast and precise detection of mentioned biological elements in a very simple and efficient configuration with remarkable specifications (sensitivity, DL, FOM and Q-factor) can be stated as the advantages and novelties of the proposed structure. This work is organized in 3 sections. The first is attained to the physical principle and methodology. The second one considers the simulations and results and the final section discusses the conclusions.

Physical principle

The proposed PhC based device is made of 28*25 rods made of silicon (situated in air medium). PhC designation is in the form of situating silicon rods in air background. In order to calculate and extract PBG and field distribution spectra, Maxwell's equations can be utilized (for evaluating applicability of designed device)[36]:

$$\Delta \times H = \frac{\partial D}{\partial t} + j_e \tag{1}$$

$$\Delta \times E = -\frac{\partial B}{\partial t} - j_m \tag{2}$$

In which E (electric field), H (magnetic field), D (displacement) and B (magnetic induction). j_e and j_m stand for electric and magnetic current sources.

$$D(x,z,t) = \varepsilon_0 \varepsilon_r(x,z) E(x,z,t) \tag{3}$$

$$B(x,z,t) = \mu_0 H(x,z,t) \tag{4}$$

where ε_r (relative permittivity of the material), ε_0 (permeability) and μ_0 (permittivity).

PWE and FDTD are the numerical techniques which are used for producing PBG and field distribution spectra[37]. As known, some parameters are essential for investigating properties of a designed sensor. Quality factor is a useful biosensing defining parameter[38].

$$Q = \frac{\lambda_0}{\Delta\lambda_{FWHM}} \tag{5}$$

in which λ_0 is the resonant wavelength and $\Delta\lambda_{FWHM}$ is the spectral with of half maximum for the central transmission spectrum. Sensitivity (S) also defines sensor's application.

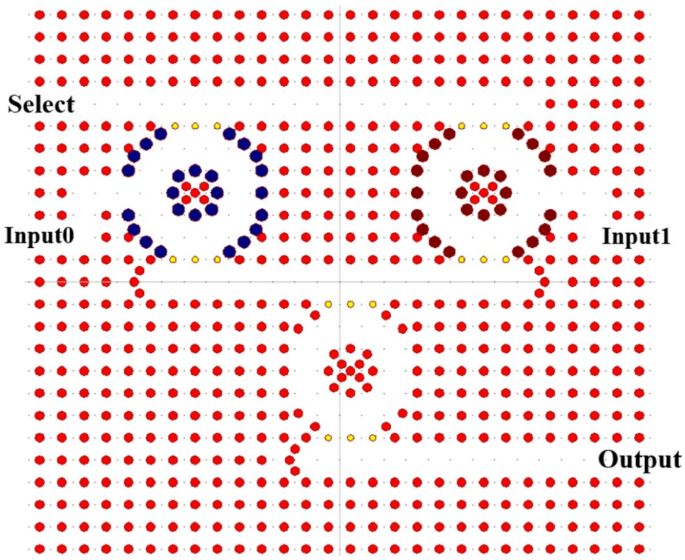

Fig. 1. Designed 2-D PhC structure.

Parameter	Value
Red rod's radius	0.1 µm
Dark blue rod's radius	0.14 µm
Dark red rod's radius	0.12 µm
Yellow rod's radius	0.08 µm
Lattice constant (a)	0.45 µm
Refractive index of rods	3.5
Refractive index of air	1

Table 1. Geometrical parameters of Fig. 1

$$S = \frac{\Delta\lambda}{\Delta n}(\mathrm{nm/RIU}) \tag{6}$$

In which $\Delta\lambda$ and Δn stand for displacement of transmission spectra and RI variation. Detection limit (DL) which indicates the lowest possible detecting amount is also an important parameter shown in Eq. (7).

$$DL = \frac{\lambda}{10SQ}(\mathrm{RIU}) \tag{7}$$

λ, S and Q indicate the wavelength related to resonance, S and Q parameters, respectively.

Another vital factor is *FOM*.

$$FOM = \frac{SQ}{\lambda}(\mathrm{RIU}^{-1}) \tag{8}$$

λ, S and Q represent wavelength, S and Q parameters, respectively[38].

Designed PhC structure is depicted in Fig. 1

A 2:1 PhC based MUX based on 28*25 silicon rods in air medium is presented in Fig. 1. Refractive indices of silicon and air are 3.5 and 1, respectively. In designed structure, linear rods are considered for facilitating the fabrication and designation processes. In the presented structure, point defects (rod with various radii) were considered for filtering specific wavelengths. All of the rods are made of silicon with RI = 3.5 and only their radii differ (radii are mentioned in Table 1).

As seen in Fig. 1, dark blue and dark red rod's radii are different from other rod's radii. These rods operate as confining media for sensing application (reflect rods, which are in touch with the analyte). They can filter and guide resonant wavelengths (they guide light wave with different resonant wavelengths considering select signal).

Yellow rods can also operate as the coupling rods; being able of leading applied light wave to output port (depending on the analyte, resonant wavelength and signal applied to select port, dark blue or dark red rods can confine the incident light waves of inputs 0 and 1). Geometrical factors of Fig. 1 are stated in Table 1.

State	Select	Input0	Input1	Output
1	0	0	0	0
2	0	0	1	0
3	0	1	0	1
4	0	1	1	1
5	1	0	0	0
6	1	0	1	1
7	1	1	0	0
8	1	1	1	1

Table 2. Logic table of the proposed MUX biosensor.

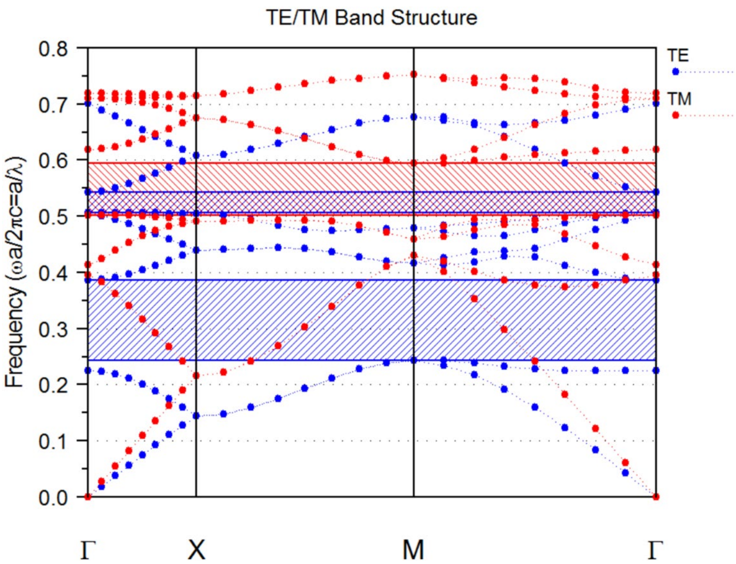

Fig. 2. Schematic of PBG of the designed system.

As known, multiplexer (MUX) is mostly referred to as data selector. MUX is a structure that can select among various conditions of input signal; guiding a specific input (according to the select port) to an output port. Therefore, in the 2:1 MUX designation, two input ports, a select and an output port are required[39]. Table 2, tabulates the logical status of designed 2:1 PhC MUX.

For studying functionality of designed system, PBG spectrum could be extracted. This spectrum indicates guided and non-guided band gap regions. PBG diagram is seen in Fig.2.

As indicated in Fig. 2, TE (Transverse Electric) and TM (Transverse Magnetic) modes could be calculated for proposed 2:1 MUX. TE modes can be achieved in wavelength region of 1.25 μm $< \lambda <$ 2.08 μm and 0.909 μm $< \lambda <$ 1 μm. TM modes can be achieved in wavelength region of 0.83 μm $< \lambda <$ 1 μm. As shown in Fig. 2, TE PBG are the most dominant ones due to their wider wavelength regions. Therefore, further simulations would be conducted considering TE PBG wavelength ranges (in these wavelengths, signal can be guided along waveguides according to TIR effect). TIR effect happens when signal with wavelengths situated in TE PBG range would be applied to the structure. In these wavelengths, signal would be reflected after hitting each rod (propagating along the waveguide). Thus, very low amounts of input signal would be dispersed (wavelengths situated in TE PBG mode ranges). For evaluating characteristics of the designed system (Fig. 1) as a biosensor (2:1 MUX) for detection of cholesterol (diagnosis of hypercholesterolemia) and creatinine (diagnosis of acute kidney injuries), simulations considering various wavelengths (central wavelength of the light wave) would be conducted. It should be noted that, proposed structure would be simulated by RSoft Photonic Device Tools. In order to simulate the system, Full-Wave and Band-Solve modules would be utilized. The Band-Solve module considering PWE method would be applied for generating band structures. The Full-Wave module considering FDTD method would also be used for calculating field distribution. In FDTD simulation, Δt (time step that should be less than $\lambda/10$), and $\Delta x = \Delta z$ (mesh sizes in both x and z directions) are considered as 0.2 fs and 100 nm, respectively. It should also be stated that, blood samples would be considered as analyte. Analyte would be introduced considering their refractive indices (as known, blood samples include various elements like cholesterol and creatinine; which have specific refractive indices for different concentrations). Finally, considering the obtained results, concentrations of specific blood components could be detected.

In the following sections, simulation at various wavelengths (situated in the TE PBG range) would be considered. Signal with $\lambda = 1300$ nm would be applied to the select port (according to Table 2). In order to consider different states mentioned at Table 2, signals with $\lambda = 1580$ nm, $\lambda = 1890$ nm, would be applied to the system. Finally, detection of cholesterol and creatinine would be considered. In the last step, important bio-sensing parameters (*Q*, *S*, *DL* and *FOM*) would be calculated.

Simulations and results

In the current section, functionality of the designed structure would be studied (states mentioned in Table 2 will be testified). Field distribution and transmission diagrams for various wavelengths (of incident light wave) would be considered. The first state of table 0.2 (Select (S) = 0, Input0 (I_0) = 0, Input1 (I_1) = 0) wouldn't lead to signal propagation. Thus, no output would be obtained. Therefore, states 2 to 8 would be investigated.

S = 0, I_0 = 0, I_1 = 1

The second state of Table 2 is S = 0, I_0 = 0, I_1 = 1, which would be considered in this part. For studying functionality of designed system at this state, incident field with $\lambda = 1890$ nm (which is in the TE PBG region) would be applied to I_1 port. Field distribution spectrum can be seen in Fig. 3.

According to Table 2 and functionality principle of 2:1 MUX, when S = 0, signals applied to I_0 would be transferred to output port. As a result, by considering state # 2, (I_0 = 0), no signal is propagated in the waveguide. Therefore, no signal is transmitted to output port.

S=0, I_0=1, I_1=0

The third state of Table 2 is S = 0, I_0 = 1, I_1 = 0, which would be studied in this section. For studying functionality of designed system at this state, input signal with $\lambda = 1580$ nm (which is in the TE PBG region) would be inserted to I_0 port. Field distribution diagram is depicted in Fig. 4.

According to Table 2 and functionality principle of 2:1 MUX, when S = 0, signals applied to I_0 would be transmitted to output port. Thus, for state # 3 (I_0 = 1), incident light wave would be propagated in the waveguide. Result is in accordance with truth table (Table 2). This state of 2:1 MUX can be considered for bio-sensing application. Thus, designed system can be applied in bio-optical OICs. For this purpose, various concertation of cholesterol in blood would be introduced as the analyte[32]. Transmission-wavelength spectrum can be seen in Fig. 5.

As mentioned, high concentrations of cholesterol might lead to hypercholesterolemia (increase risks of heart diseases and strokes). As seen in Fig. 5, this structure can help detect cholesterol levels in blood samples. RIs of different Cholesterol levels in blood can be considered as ($n = 2.59$ for 200 mg/dl, $n = 2.62$ for 220 mg/dl, $n = 2.80$ for 240 mg/dl and $n = 3.06$ for 260 mg/dl)[32].

As known, appropriate cholesterol levels must be less than 200 mg/dl (5.17 mmol/L). Therefore, cholesterol level higher than 200 mg/dl can cause risks of different diseases[32,40]. As depicted in Fig. 5, enhancing RI increases peak wavelength of transmission diagram (wavelength is red-shifted)[41,42].

Resonant wavelength shift occurs due to the dependency of analyte's RI to position. In fact, mobility can be defined by the condition of standing wave[31]. Following equation indicates this dependency.

$$\Delta = m\lambda = nG \tag{9}$$

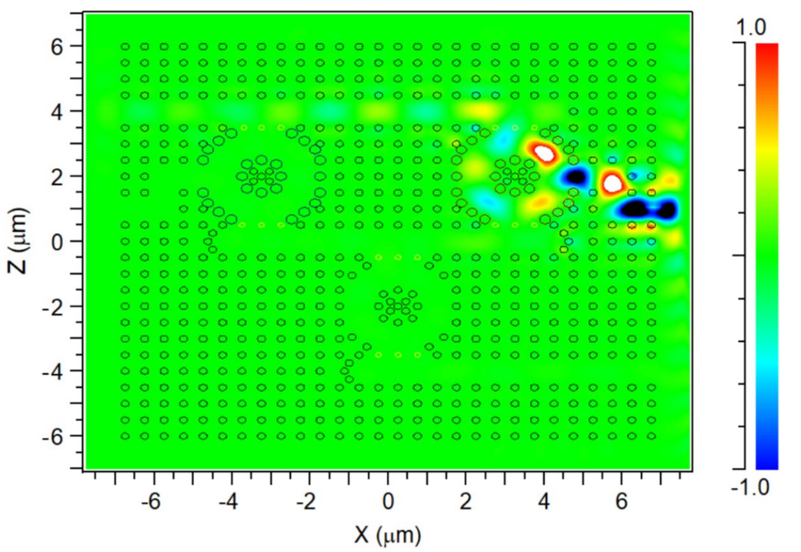

Fig. 3. View of field distribution for state #2.

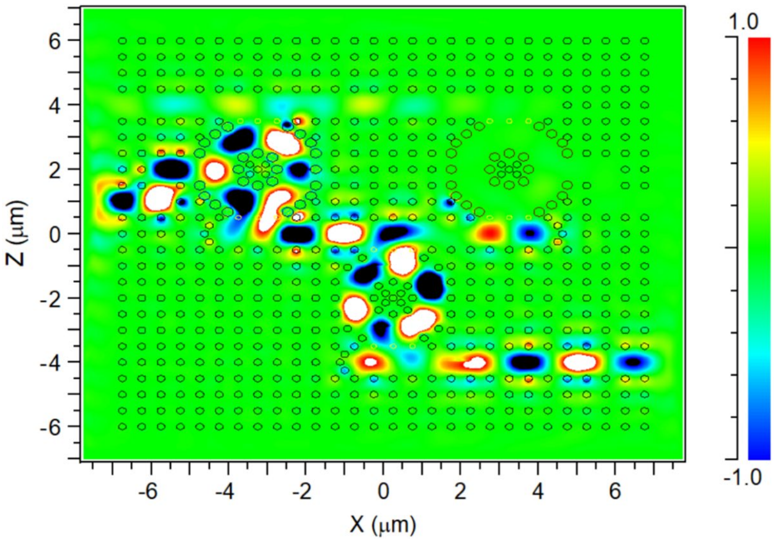

Fig. 4. View of field distribution for state #3.

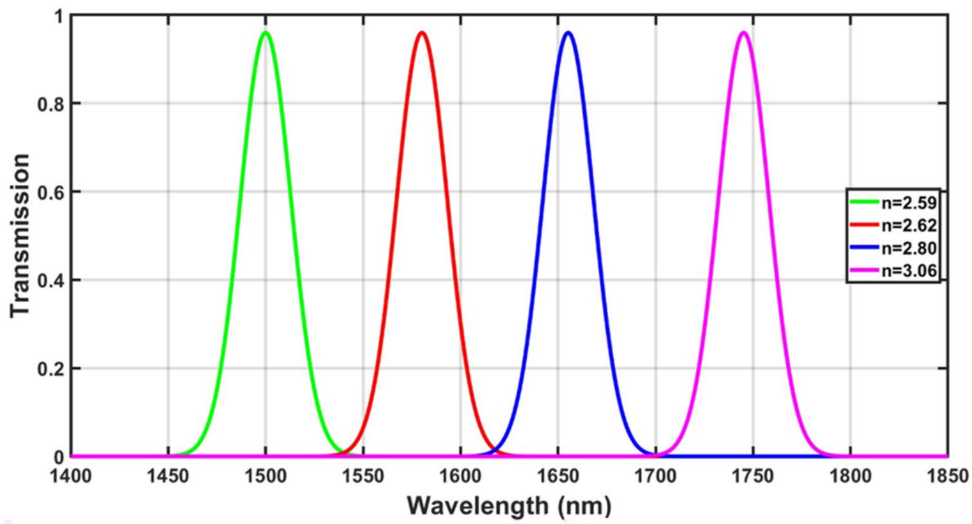

Fig. 5. Transmission-wavelength spectrum for different cholesterol concentrations.

in which Δ (path difference), m (integer), n (RI) and G (geometric path difference). According to Eq. 9, by increasing n (refractive index of analyte), λ (transmission wavelength) would also be increased (as shown in Fig. 5).

Important factors indicating functionality of a sensor are calculated in the following part.

Q: (45.4–52.88), *S*: 2673.4 nm/RIU, *DL*: (0.00125–0.00143) RIU, *FOM*: (80.91–82.06) RIU^{-1}. Considering obtained results, designed 2:1 MUX at mentioned state can be utilized as an efficient biosensor and can help physicians in early and precise prognosis of hypercholesterolemia.

S = 0, I_0 = 1, I_1 = 1

The fourth state of Table 2 is S = 0, I_0 = 1, I_1 = 1, that would be investigated in this section. In order to study functionality of designed system at this state, signals with λ = 1890 nm and λ = 1580 nm would be inserted to I_1 and I_0 ports. Field distribution diagram is shown in Fig. 6.

According to Table 2 and functionality principle of 2:1 MUX, when S = 0, signals inserted to I_0 would be transmitted to output port. Therefore, by considering state # 4, (I_0 = 1), input field would be transferred to output port. Result is in accordance with truth table (Table 2).

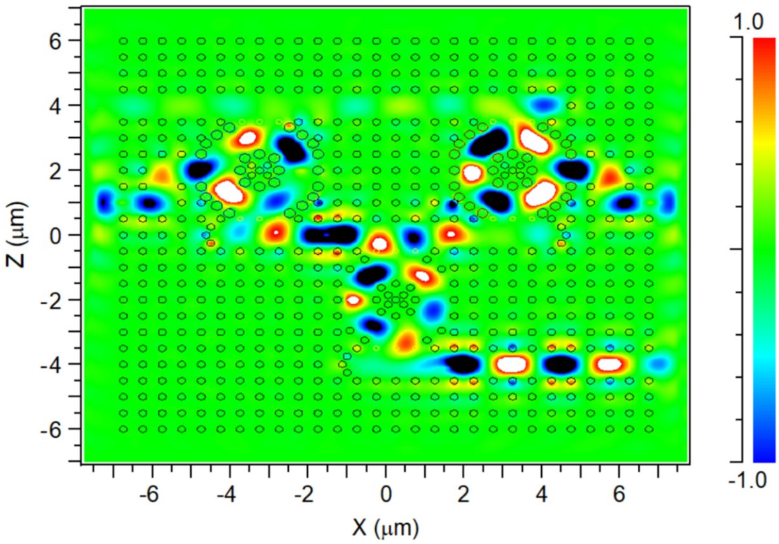

Fig. 6. Schematic of field distribution for state #4.

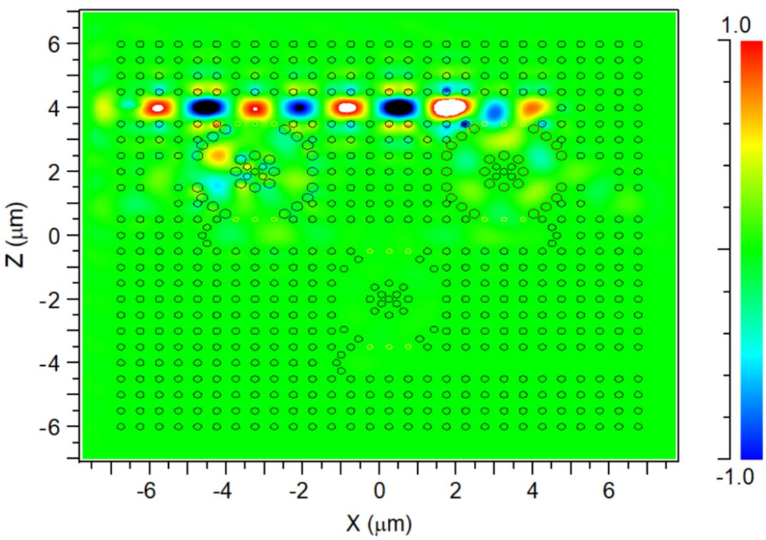

Fig. 7. Schematic of field distribution for state #5.

S=1, I_0=0, I_1=0

The fifth state of Table 2 is S = 1, I_0 = 0, I_1 = 0, that would be studied in this section. For studying functionality of designed system at this state, incident field with $\lambda = 1300$ nm (which is in the TE PBG region) would be applied to S port. Field distribution diagram is depicted in Fig. 7.

According to Table 2 and functionality principle of 2:1 MUX, when S = 1, signals applied to I_1 would be propagated in the structure. Thus, by considering state # 5, (I_1 = 0), no signal is propagated in the waveguide. Therefore, as seen in Fig. 7, no signal is transmitted to output port.

S=1, I_0=0, I_1=1

The sixth state of Table 2 is S = 1, I_0 = 0, I_1 = 1, that is considered in this part. In order to investigate functionality of designed system at this state, signals at $\lambda = 1890$ nm and $\lambda = 1300$ nm would be applied to I_1 and S ports, respectively. Field distribution diagram is depicted in Fig. 8.

As previously mentioned, in a 2:1 MUX, when S = 1, signals applied to I_1 would be transferred to output port. As a result, by considering state #6, (I_1 = 1), incident light wave would be propagated in the waveguide. Result is in accordance with truth table (Table 2). This state of 2:1 MUX can be utilized for bio-sensing application. Therefore, designed system can be applied in bio-optical OICs. For this purpose, different amounts of creatinine in blood samples would be introduced as the analyte. Transmission-wavelength diagram is shown in Fig. 9.

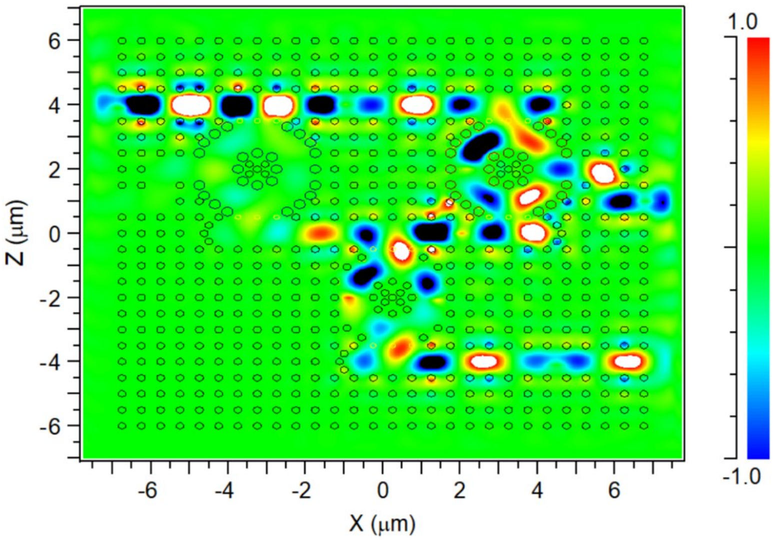

Fig. 8. Schematic of field distribution for state #6.

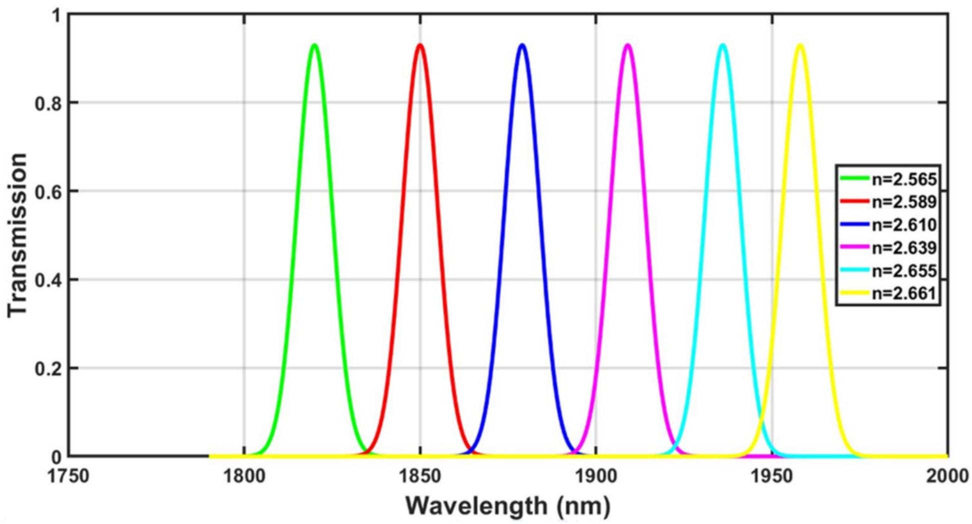

Fig. 9. Transmission-wavelength spectrum for different creatinine concentrations.

RIs utilized in Fig. 9b as 2.565, 2.589, 2.610, 2.639, 2.655 and 2.661 are related to different concentrations of creatinine in blood ($n = 2.565$ for 85.28 μmol/L, $n = 2.589$ for 84.07 μmol/L, $n = 2.610$ for 83.3 μmol/L, $n = 2.639$ for 82.3 μmol/L, $n = 2.655$ for 81.43 μmol/L and $n = 2.661$ for 80.9 μmol/L[31]). As can be seen in Fig. 9, RI increment can shift peak wavelength to higher values[41,42]. According to Fig. 9 and Eqs. (5–8), following biosensing parameters can be calculated. *Q*: (101.1–109.4), *S*: 3582.7 nm/RIU, *DL*: (4.98e−4–5.26e−4) RIU, *FOM*: (199.01–201.3) RIU^{-1}. Considering designed structure at state #6, acute kidney injuries can be effectively diagnosed by physicians in early stages.

S=1, I_0=1, I_1=0

The seventh state of Table 2 is S = 1, $I_0 = 1$, $I_1 = 0$, which is studied in this section. For studying functionality of designed system at this state, incident fields at $\lambda = 1580$ nm and $\lambda = 1300$ nm would be inserted to I_0 and S ports. Field distribution spectrum is shown in Fig. 10.

According to Table 2 and functionality principle of 2:1 MUX, when S = 1, signals inserted to I_1 would be transmitted to output port. Therefore, in this case, ($I_1 = 0$), no signal is transferred to output port. Obtained result is in accordance with truth table (Table 2).

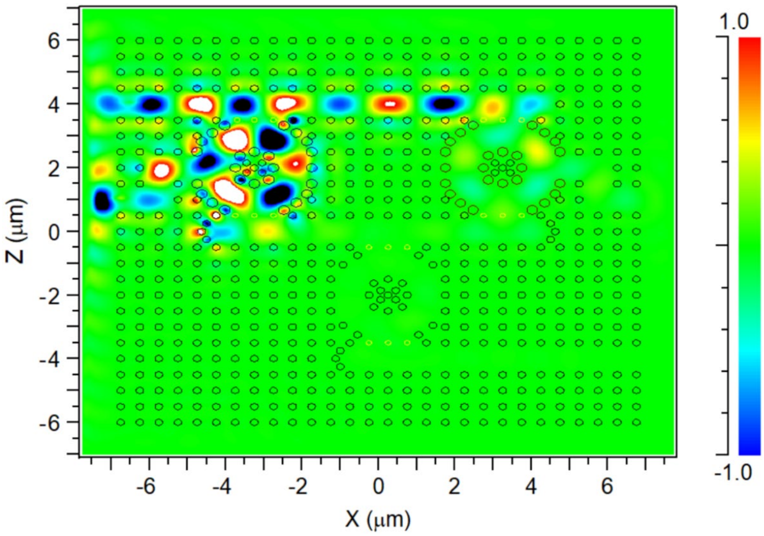

Fig. 10. View of field distribution for state #7.

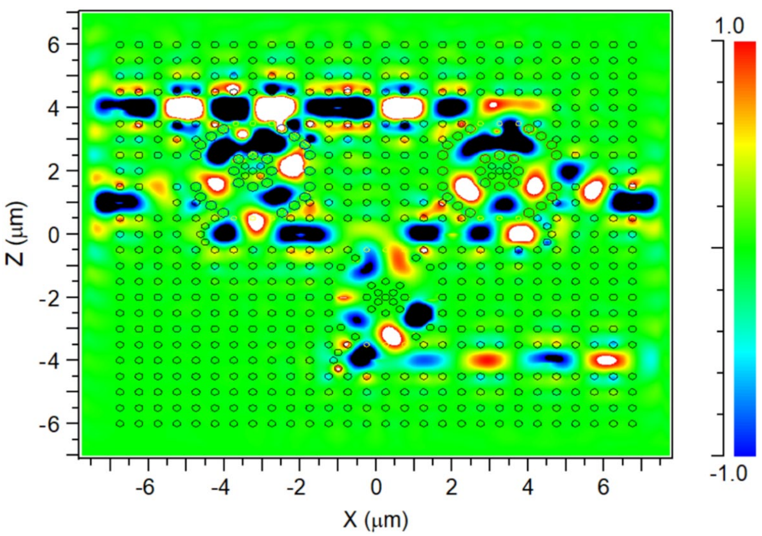

Fig. 11. View of field distribution for state #8.

S=1, I_0=1, I_1=1

The eighth state of Table 2 is S = 1, $I_0 = 1$, $I_1 = 1$, that is investigated in this section. For studying functionality of designed system at this state, signals with $\lambda = 1890$ nm, $\lambda = 1580$ nm and $\lambda = 1300$ nm would be applied to I_1, I_0 and S ports. Field distribution diagram is shown in Fig. 11.

According to Table 2 and functionality principle of 2:1 MUX, when S = 1, signals applied to I_1 would be transferred to output port. Therefore, for this case, signal applied to I_1 would be transmitted in the structure. As seen, all of 2:1 MUX states mentioned in Table 2, were considered in designed system (obtained results were similar to Table 2). Moreover, two states were utilized as biosensors with considerable bio-sensing factors for detection of cholesterol and creatinine. Therefore, designed structure can be an appropriate candidate for bio-sensing applications in OICs. In order to indicate functionality of designed system, obtained results of proposed structure (as biosensors for detection of cholesterol and creatinine) are compared with previously reported works. Results are tabulated in Table 3.

Conclusion

In the presented work, an efficient ring-shaped PhC based biosensor made of 28*25 silicon rods was proposed. Proposed structure was designed in the form of three ring-shaped waveguides and was supposed to function as a 2:1 MUX. In the designation process, circumferences of two upper ring-shaped PhCs were covered by dark blue and dark red rods (with different radii) for fulfilling interfering and scattering phenomena. These phenomena occurred due to TIR effect; guiding incident light waves to output port. The whole structure was then considered

References	Sensitivity (nm/RIU)	FOM (RIU^{-1})	Q-factor	LOD (RIU)
Cholesterol sensor[32]	469	125		0.0091
Cholesterol sensor[43]	156.18	10.41	19	0.008
Cholesterol sensor[44]	245.6714	13.5	28	0.0063
Our proposed cholesterol sensor	2673.4	80.91–82.06	45.4–52.88	0.00125–0.00143
Creatinine sensor[35]	1562.5	78.125	51	6.4e−4
Creatinine sensor[31]	306.25	150	97	5e−4
Creatinine sensor[45]	637	10.3	89	6e−4
Our proposed creatinine sensor	3582.7	199.01–201.3	101.1–109.4	4.98e−4–5.26e−4

Table 3. Comparison of our proposed sensors with previous works.

as a biosensor for detecting various concentrations of cholesterol and creatinine in blood samples. By inserting a drop of blood sample in the structure and applying signals to Input0, Input1 and Select ports (in specific conditions), various concentrations of cholesterol and creatinine could be detected. The simulation process for obtaining PBG and field distribution diagrams were conducted by considering PWE and FDTD methods in RSoft Photonic Device Tools. Finally, bio-sensing parameters of the proposed structure were calculated and reported. For cholesterol by considering ($I_0=1$, $I_1=0$ and $S=0$), *Q*: (45.4–52.88), *S*: 2673.4 nm/RIU, *DL*: (0.00125–0.00143) RIU and *FOM*: (80.91–82.06) RIU^{-1} were calculated. For creatinine, by considering ($I_0=0$, $I_1=1$ and $S=1$), *Q*: (101.1–109.4), *S*: 3582.7 nm/RIU, *DL*: (4.98e−4–5.26e−4) RIU and *FOM*: (199.01–201.3) RIU^{-1} were obtained. Designed structure could be an appropriate candidate for bio-sensing applications (early and precise diagnosis of various diseases related to cholesterol and creatinine) in bio- optoelectronic systems.

Data availability

All data generated or analysed during this study are included in this published article.

Received: 12 March 2025; Accepted: 5 May 2025
Published online: 15 May 2025

References

1. Mohammed, N. A. et al. Tuberculosis biomedical sensor based on on-chip nanocavity 2D photonic crystal with high sensitivity and quality factor. *Measurement* **222**, 113595 (2023).
2. Wang, Y. et al. A wearable platform for biochemical sweat analysis using photonic crystal hydrogel. *Anal. Chim. Acta.* **1338**, 343590 (2025).
3. Parandin, F. & Sheykhian, A. Design and simulation of a 2 × 1 All-Optical multiplexer based on photonic crystals. *Opt. Laser Technol.* **151**, 108021 (2022).
4. Rafiee, E. & Emami, F. Design of a novel all-optical ring shaped demultiplexer based on two-dimensional photonic crystals. *Optik* **140**, 873–877 (2017).
5. Parandin, F. High contrast ratio all-optical 4 × 2 encoder based on two-dimensional photonic crystals. *Opt. Laser Technol.* **113**, 447–452 (2019).
6. Khani, S. et al. High resolution refractive index and temperature sensor with Fano resonance in disk and parenthesis-shaped plasmonic cavities. *Results Opt.* **19**, 100816 (2025).
7. Chowdhury, K. H. et al. Sensing the future with graphene-based wearable sensors: A review. *Results Mater.* **25**, 100646 (2025).
8. Lotfi, F. et al. Resonator-based nanoscale plasmonic sensor made of metal–graphene–insulator interfaces. *Results Phys.* **64**, 107922 (2024).
9. Ouerghi, F. et al. Multiplex biomolecules-sensing: Simulation of an ultrasensitive sensor array for disease diagnosis via two-dimensional photonic crystals. *Opt. Laser Technol.* **188**, 112899 (2025).
10. Rafiee, E. et al. Design of a novel nano plasmonic-dielectric photonic crystal power splitter suitable for photonic integrated circuits. *Optik* **172**, 234–240 (2018).
11. Parandin, F., Kamarian, R. & Jomour, M. A novel design of all optical half-subtractor using a square lattice photonic crystals. *Opt Quant Electron.* **53**, 114 (2021).
12. Parandin, F. et al. Design of 2D photonic crystal biosensor to detect blood Components. *Opt Quant Electron.* **54**, 618 (2022).
13. Zayets, V. et al. Fabrication technique for low-loss plasmonic waveguides incorporating both "plasmonic-friendly" and "plasmonic-unfriendly" metals. *Photonics Nanostruct.* **57**, 101196 (2023).
14. Ahmadianyazdi, A. et al. Glucose measurement via Raman spectroscopy of graphene: Principles and operation. *Nano Res.* **15**, 8697–8704 (2022).
15. Fathi, F. et al. Inverse opal photonic crystals: Recent advances in fabrication methods and biological applications. *J. Drug Deliv. Technol.* **72**, 103377 (2022).
16. Bhandarkar, S. PHOTONIC CRYSTALS | self-assembled and functionalized photonic crystals. In *Encyclopedia of Modern Optics* 155–164 (2005).
17. Shen, P. et al. Three-dimensional/two-dimensional photonic crystal hydrogels for biosensing. *J. Mater. Chem. C.* **9**, 5840–5857 (2021).
18. Sovizi, M. et al. Highly sensitive simultaneous measurement of refractive index and its changes using a photonic crystal biosensor with coupled resonators. *Results Phys.* **70**, 108179 (2025).
19. Palai, G. et al. Optical MUX/DEMUX using 3D photonic crystal structure: A future application of silicon photonics. *Optik* **128**, 224–227 (2017).
20. Vahdati, A. & Parandin, F. Antenna patch design using a photonic crystal substrate at a frequency of 1.6 THz. *Wireless Pers. Commun.* **109**, 2213–2219 (2019).
21. Parandin, F. & Moayed, M. Designing and simulation of 3-input majority gate based on two-dimensional photonic crystals. *Optik* **216**, 164930. https://doi.org/10.1016/j.ijleo.2020.164930 (2020).

22. Parandin, F. Ultra-compact terahertz all-optical logic comparator on GaAs photonic crystal platform. *Opt. Laser Technol.* **144**, 107399. https://doi.org/10.1016/j.optlastec.2021.107399 (2021).
23. Parandin, F., Heidari, F., Rahimi, Z. & Olyaee, S. Two-dimensional photonic crystal biosensors: A review. *Opt. Laser Technol.* **144**, 107397. https://doi.org/10.1016/j.optlastec.2021.107397 (2021).
24. Askarian, A. Design and analysis of all optical 2 × 4 decoder based on Kerr effect and beams interference procedure. *Opt Quant Electron* **53**, 291 (2021).
25. Parandin, F. et al. A comprehensive review of blood component detection utilizing one-dimensional, two-dimensional, and photonic crystal fiber biosensors. *Results Opt.* **16**, 100671 (2024).
26. Peng, W. et al. A flexible and stretchable photonic crystal sensor for biosensing and tactile sensing. *Heliyon* **8**, e11697 (2022).
27. Rheima, A. H. et al. Nano biosensors: Classification, electrochemistry, nanostructures, and optical properties. *Results Eng.* **24**, 103428 (2024).
28. Rafiee, E. et al. Hypercholesterolemia diagnosis by a biosensor based on photonic crystal PANDA structure. *Opt Rev.* **31**, 87–93 (2024).
29. Tasnim, N. et al. Highly sensitive photonic crystal fiber based surface plasmon resonance biosensor for detection of wide range of organic solutions. *Sens. Bio Sens. Res.* **43**, 100623 (2024).
30. Panda, A. et al. Performance analysis of graphene-based surface plasmon resonance biosensor for blood glucose and gas detection. *Appl. Phys. A* https://doi.org/10.1007/s00339-020-3328-8 (2020).
31. Aly, A. H., Mohamed, D., Mohaseb, M. A., Abd El-Gawaad, N. S. & Trabelsi, Y. Biophotonic sensor for the detection of creatinine concentration in blood serum based on 1D photonic crystal. *RSC Adv.* **10**, 31765. https://doi.org/10.1039/D0RA05448H (2020).
32. Dash, D. & Saini, J. Hyperbolic graded index biophotonic cholesterol sensor with improved sensitivity. *Prog. Electromagn. Res. M* **116**, 165–176 (2023).
33. Rahman, M. et al. Photonic crystal fiber based terahertz sensor for cholesterol detection in human blood and liquid foodstuffs. *Sens. Bio Sens. Res.* **29**, 100356 (2020).
34. Kumar, A. et al. Ultrahigh sensitive graphene oxide/conducting polymer composite based biosensor for cholesterol and bilirubin detection. *Biosens. Bioelectron. X* **13**, 100290 (2023).
35. Negahdari, R. et al. Sensitive MIM plasmonic biosensors for detection of hemoglobin, creatinine and cholesterol concentrations. *Diam. Relat. Mater.* **136**, 110029 (2023).
36. Karkhanehchi, M. M., Parandin, F. & Zahedi, A. Design of an all-optical half-adder based on 2D photonic crystals. *Photonic Netw. Commun.* **33**, 159 (2017).
37. Gao, Y. F. et al. Design of novel power splitters by directional coupling between photonic crystal waveguides. *Optoelectron. Lett.* **6**, 417–420. https://doi.org/10.1007/s11801-010-0017-4 (2010).
38. Olyaee, S. et al. Two-curve-shaped biosensor using photonic crystal nano-ring resonators. *JNS* **4**, 303–308 (2014).
39. Richard, J. et al. Multiplexer theory and design. In *Microwave Filters for Communication Systems: Fundamentals, Design, and Applications* 569–608 (Wiley, 2018).
40. Ma, H. Cholesterol and human health. *Nat. Sci.* **2**(4), 17–21 (2004).
41. Chorsi, H. T. et al. Tunable plasmonic substrates with ultrahigh Q-factor resonances. *Sci. Rep.* **7**, 15985 (2017).
42. Chahkoutahi, A. et al. Sensitive hemoglobin concentration sensor based on graphene-plasmonic nano-structures. *Plasmonics* **17**, 423–431 (2022).
43. Lu, Y. et al. Beta-cyclodextrin based reflective fiber-optic SPR sensor for highly-sensitive detection of cholesterol concentration. *Opt. Fiber Technol.* **56**, 102187. https://doi.org/10.1016/j.yofte.2020.102187 (2020).
44. Fu, X. et al. High sensitivity refractive index sensor based on cascaded core-offset splicing NCF-HCF-NCF structure. *Opt. Fiber Technol.* **68**, 102791 (2022).
45. Gandhi, S., Awasthi, S. K. & Aly, A. H. Biophotonic sensor design using a 1D defective annular photonic crystal for the detection of creatinine concentration in blood serum. *RSC Adv.* **11**, 26655–26665 (2021).

Author contributions
"Esmat Rafiee" contributed to the study conception and design. Material preparation, data collection and analysis were performed by "Esmat Rafiee". The manuscript was written by "Esmat Rafiee".

Funding
The authors declare that no funds, grants, or other support were received during the preparation of this manuscript.

Declarations

Competing interests
The authors declare no competing interests.

Additional information
Correspondence and requests for materials should be addressed to E.R.

Reprints and permissions information is available at www.nature.com/reprints.